https://doi.org/10.5194/hess-2024-71
Preprint. Discussion started: 29 April 2024

Hydrology and Earth System Sciences
Open Access
Discussions

A novel framework for accurately quantifying wetland depression water storage capacity with coarse-resolution terrain data

Boting Hu[1,2], Liwen Chen[1], Yanfeng Wu[1], Jingxuan Sun[1,2], Y. Jun Xu[3], Qingsong Zhang[1,2], Guangxin Zhang[1]

[1] Northeast Institute of Geography and Agroecology, Chinese Academy of Sciences, Changchun, Jilin 130102, China

[2] University of Chinese Academy of Sciences, Beijing 100049, China

[3] School of Renewable Natural Resources, Louisiana State University Agricultural Center, 227 Highland Road, Baton Rouge, LA 70803, USA

Correspondence to: Guangxin Zhang (zhgx@iga.ac.cn)

Abstract. Accurate quantification of wetland depression water storage capacity (WDWSC) is imperative for comprehending the wetland hydrological regulation functions to support integrated water resources management. Considering the challenges posed by the high acquisition cost of high-resolution LiDAR DEM or the absence of field measurements for most wetland areas, urgent attention is required to develop an accurate estimation framework for WDWSC using open-source, low-cost, multi-source remote sensing data. In response, we developed a novel framework, WetlandSCB, utilizing coarse-resolution terrain data for accurate estimation of WDWSC. This framework overcame several technical difficulties, including biases in above-water topography, incompleteness and inaccuracy of wetland depression identification, and the absence of bathymetry. Validation and application of the framework were conducted in two national nature reserves of northeast China. The study demonstrated that integrating priority-flood algorithm, morphological operators and prior information can accurately delineate the wetland depression distribution with overall accuracy and Kappa coefficient both exceeding 0.95. The use of water occurrence map can effectively correct numerical biases in above-water topography with Pearson coefficient and R^2 increasing by 0.33 and 0.38 respectively. Coupling spatial prediction and modeling with remote sensing techniques yielded highly accurate bathymetry estimates, with <3% relative error compared to filed measurements. Overall, the WetlandSCB framework achieved estimation of WDWSC with <10%

relative error compared to field topographic and bathymetric measurements. The framework and its concept are transferable to other wetland areas globally where field measurements and/or high-resolution terrain data are unavailable, contributing to a major technical advancement in estimating WDWSC in river basins.

Keywords: Wetland depression; Water storage capacity; Hypsometric curve; coarse-resolution terrain data; wetland hydrological regulation functions

1 Introduction

Wetlands are multifunctional ecosystems considered as nature-based solutions for effective water management in river basins (Thorslund et al., 2017). They exert a profound influence on watershed hydrological processes and water resource availability through their hydrological regulation functions, such as maintaining baseflow, buffering floods, and delaying droughts (Acreman and Holden, 2013; Wu et al., 2023). These functions are essential for enhancing watershed resilience and ensuring water security (Cohen et al., 2016; Evenson et al., 2018; Lane et al., 2018). Wetland depression water storage capacity (hereafter abbreviated as WDWSC) represents a critical component of wetland hydrological regulation functions. The quantitative study of the WDWSC to advance scientific insights into wetland hydrological regulation functions and support integrated water resources management (Ahmad et al., 2020; Fang et al., 2019; Jones et al., 2018; Shook et al., 2021).

The WDWSC can be defined as the maximum surface water volume that each wetland depression can store without spilling to down-gradient waters (Jones et al., 2018). Previous studies predominantly employed wetland depression identification algorithms to derive wetland depression topography from terrain data. Subsequently, hypsometric curves (area-depth) are constructed based on the derived topography. Finally, the integration of the hypsometric curves is solved to determine the WDWSC (e.g., Haag et al., 2005; Wu and Lane, 2016). Therefore, the key determinants for the accuracy of the WDWSC calculation are the rationality of the wetland depression identification algorithms and the precision of terrain data. Many scholars have conducted research on wetland depression identification algorithms, which can be mainly categorized into three types: depression filling, depression breaching and hybrid combing both the filling and breaching approaches. Among these, the priority-flood algorithm within the depression filling category is widely adopted as a prevalent algorithm for wetland depression identification (Barnes et al., 2014; Lindsay, 2016; Wu et al., 2019; Zhou et al., 2016). The

https://doi.org/10.5194/hess-2024-71
Preprint. Discussion started: 29 April 2024

priority-flood algorithm works by flooding DEM cells inwards from their edges using a priority queue to determine the sequence of cells to be flooded. Wu et al. (2019) and Rajib et al. (2019) demonstrated the feasibility of accurately deriving wetland depression topography using the priority-flood algorithm in the Pipestem watershed and Upper Mississippi river basin, respectively. Bare-earth high-resolution airborne light detection and ranging (LiDAR) DEM can provide accurate topographic information of wetland depressions, significantly improving the estimation accuracy of the WDWSC. For example, Jones et al. (2018) used high-resolution LiDAR DEM to estimate WDWSC in the Delmarva Peninsula. However, the high acquisition cost of LiDAR DEM renders it impractical for large-scale estimation of WDWSC. The global open-access spaceborne-derived DEMs (hereafter referred as global DEMs), such as Shuttle Radar Topography Mission (SRTM), ALOS Global Digital Surface Model, the Terra Advanced Spaceborne Thermal Emission and Reflection Radiometer (ASTER) Global Digital Elevation Model, offer topographic information at a fine spatial scale. However, compared to the bare-earth LiDAR DEM, the global DEMs exhibit three obvious limitations. First, radar altimetry cannot penetrate water surfaces, so the global DEMs produced from radar altimetry do not provide any bathymetric information. Second, in certain regions, there may be substantial numerical discrepancies in above-water topography. Third, the global DEMs often suffer from lower horizontal and vertical resolutions. Due to the limitations in global DEMs, delineation of wetland depressional areas using the advanced priority-flood algorithm also suffers from three problems: the bias in above-water topography (Fig. 1a and 1b), incompleteness and inaccuracy of wetland depressions identification (Fig. 1c), and the absence of bathymetric information (Fig. 1d).

https://doi.org/10.5194/hess-2024-71
Preprint. Discussion started: 29 April 2024

Hydrology and Earth System Sciences
Open Access
Discussions

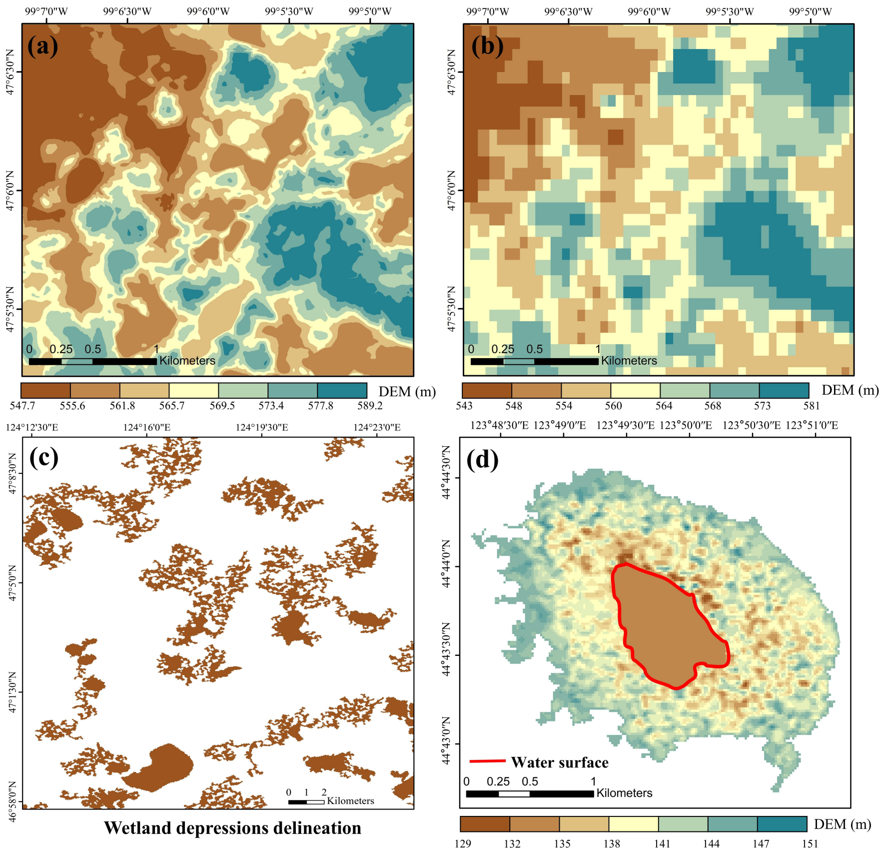

Figure 1: Wetland depression extraction based on the priority-flood algorithm and global DEMs suffers from the bias of above-water topography (Figures 1a and 1b show the discrepancies in above-water topography obtained from LiDAR DEM and ALOS DEM, respectively, in the Prairie Pothole Region of North Dakota), incompleteness and inaccuracy of wetland depressions identification (Fig. 1c), and the absence of bathymetric information (Figure 1d, where the entire water surface is represented by a single elevation value of 129 m).

In an effort to minimize the impact of the absence of bathymetric information in global DEMs on the estimation accuracy of the WDWSC, researchers have conducted studies on the estimation of underwater hypsometric relationship of wetland depressions, and the methods can be divided into two types: spatial prediction and modeling methods and remote sensing technologies. The spatial prediction and modeling methods assume that the bathymetry can be considered as a spatial extension of the

https://doi.org/10.5194/hess-2024-71
Preprint. Discussion started: 29 April 2024

surrounding exposed terrains due to long-term tectonic and geophysical evolution processes. Consequently, the underwater hypsometric relationship is assumed to be fundamentally similar to the above-water hypsometric relationship in wetland depressions (e.g., Ahmad et al., 2020; Bonnema et al., 2016; Bonnema and Hossain, 2017; Liu and Song, 2022; Tsai et al., 2010; Vanthof and Kelly, 2019; Verones et al., 2013; Wu and Lane, 2016; Xiong et al., 2021). However, the large numerical bias in the above-water topography of global DEMs in certain regions can distort the constructed above-water hypsometric relationship of wetland depressions, thus introducing significant uncertainty to the underwater hypsometric relationship estimated by this method. Over the past few decades, remote sensing technologies have demonstrated remarkable capabilities in estimating underwater hypsometric relationships at large spatial scales, facilitated by the rapid emergence of various advanced satellite sensors, including optical, passive microwave, and radar instruments (Duan and Bastiaanssen, 2013; Gao et al., 2015; Liu et al., 2022). The commonly employed approach for estimating underwater hypsometric relationship requires simultaneous observations of water area provided by optical images (e.g., Landsat series) and the corresponding water level provided by altimetry satellites (e.g., Sentinel-3, CryoSat-2, Envisat). However, accuracy challenges arise due to numerical biases of altimetry satellites, cloud contamination in some optical images, and the occasional occurrence of one water area value corresponding to multiple water level values or vice versa (Li et al., 2019a; Liu et al., 2024). In summary, previous studies have mainly utilized LiDAR DEM data to estimate WDWSC (e.g., Jones et al., 2018; Huang et al., 2011; Kessler and Gupta, 2015; Land and D'Amico, 2010; Wu et al., 2016; Wu et al., 2019). However, these studies have seriously overlooked the issues of incompleteness and inaccuracy of wetland depression identification, as well as the bias in above-water topography, resulting in a high level of uncertainty in the WDWSC estimation. In addition, insufficient attention has been paid to the drawbacks and limitations of both spatial prediction and modeling methods and remote sensing technologies in estimating bathymetry. Consequently, a comprehensive and systematic solution for the accuracy estimation of WDWSC based on the global DEMs has not yet been developed.

Therefore, this study aims to develop a framework for accurately estimating WDWSC by integrating multi-source remote sensing data and prior knowledge. Specifically, we integrated priority-flood algorithm, morphological operators and prior information on water distribution map to delineate the spatial extent of wetland depressional areas. We then corrected the bias in above-water topography based on water occurrence map. Finally, we utilized remote sensing techniques to couple

https://doi.org/10.5194/hess-2024-71
Preprint. Discussion started: 29 April 2024

spatial prediction and modeling to estimate bathymetry of wetland depressional areas. The principle contribution of this developed framework, termed as WetlandSCB, lies in addressing the challenges hindering the improvement of accuracy in estimating WDWSC based on global DEMs.

2 Methodology

The WetlandSCB framework can be summarized in four steps as illustrated in Figure 2. Step 1 delineation of wetland depressional areas; Step 2 above-water topography reconstruction; Step 3 bathymetric information estimation; and Step 4 hypsometric curve construction and WDWSC calculation. Each of the four steps are described in the following sections.

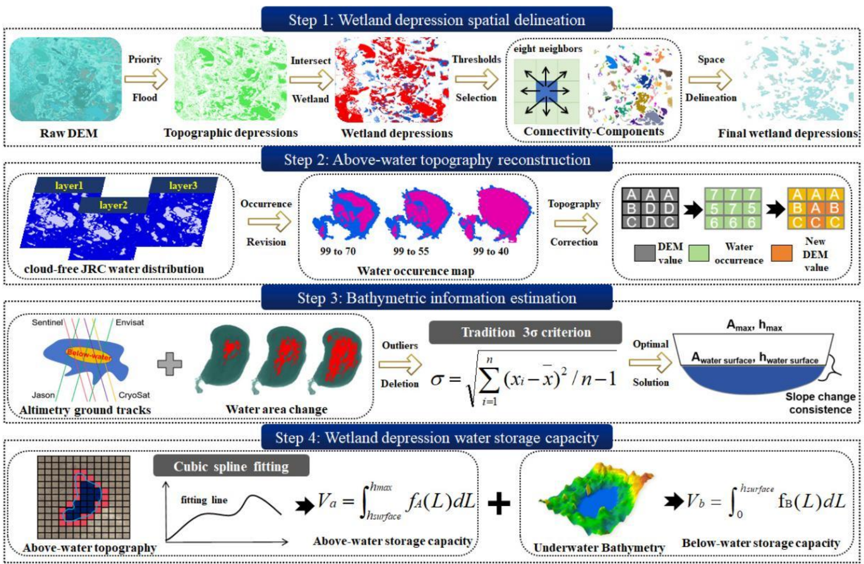

Figure 2: Flowchart of the WetlandSCB framework for accurate estimation of wetland depression water storage capacity (WDWSC) comprising four technical steps. In step 1, spatial distribution of wetland depressional areas are delineated. In step 2, wetland above-water topography is reconstruction. In step 3, bathymetric information of wetland depressional areas is estimated. In step 4, a hypsometric curve (i.e. depth-area relation) is developed and WDWSC is quantified.

2.1 Wetland depression spatial delineation

We extracted the original wetland depression map from the global DEMs based on the priority-flood algorithm and wetland maps (Fig. 3). To eliminate the artifact wetland depressions, it was necessary to transform the wetland depression map into a binary image consisting of pixels that

https://doi.org/10.5194/hess-2024-71
Preprint. Discussion started: 29 April 2024

Hydrology and Earth System Sciences
Discussions
Open Access

area labeled as logical ones (wetland depression) and zeros (non-wetland depression). We then employed the eight-neighbor connectivity algorithm to extract the spatial extent of each wetland depression from the binary image. Subsequently, the circularity (Eq. 1) and eccentricity (Eq. 2) indicators were used to exclude the artifact wetland depressions (Ahmad et al., 2020) as follows:

$$Circularity = \frac{P}{2\sqrt{\pi \cdot A}} \tag{1}$$

$$Eccentricity = \frac{D_f}{l_m} \tag{2}$$

where P (m) and A (m^2) are the perimeter and area of the wetland depression, respectively. D_f (m) and L_m (m) represent distance between foci and the length of major axis of wetland depression.

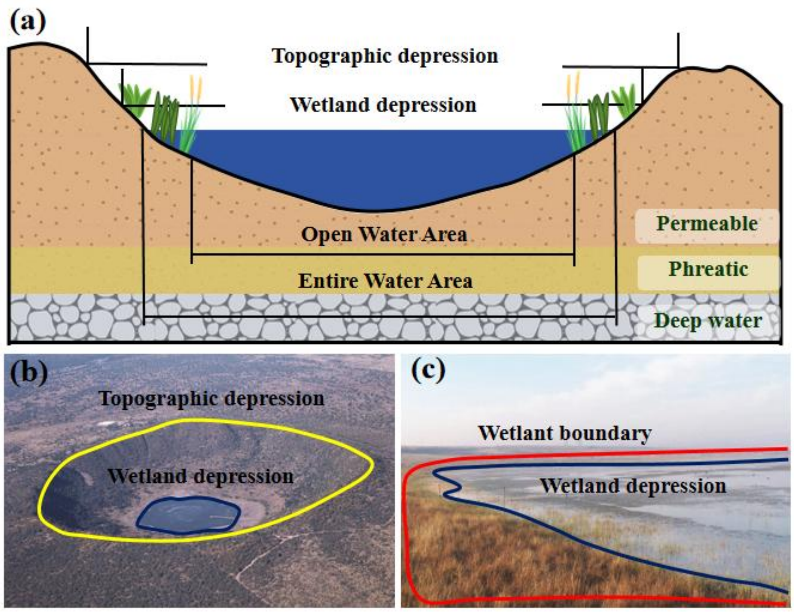

Figure 3. (a) Conceptual diagram of wetland depression profile. (b) and (c) show the two representative wetland depressional areas located in South Africa (modified from De Klerk et al., 2016).

Due to incompleteness and inaccuracy identification of some wetland depressions in the original wetland depression map (Figure 4a), morphological operators of erosion and dilation are applied for the initial spatial processes (Figure 4b). The erosion operator erodes away the boundaries of wetland depressions to enhance their edges and remove noise. The dilation operator fills up small holes (non-wetland depression pixels) surrounded by a group of wetland depression pixels (Pulvirenti et al.,

https://doi.org/10.5194/hess-2024-71
Preprint. Discussion started: 29 April 2024

Hydrology and Earth System Sciences
Discussions
Open Access

2011a). The combined effect of the two operators is to remove noises while preserving the substantive features in the image. The water distribution map, which serves as prior information, effectively characterizes the spatial extent of wetland depressions (Figure 3). Therefore, the wetland depression map, after being processed by the morphological operators, is then intersected with the water distribution map to obtain a complete and final wetland depression map (Figure 4c).

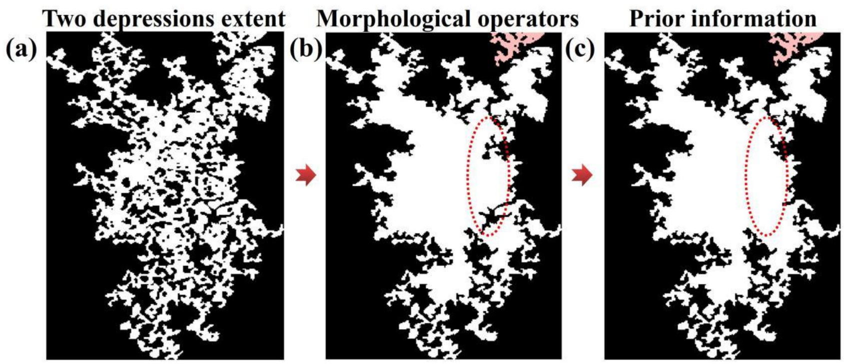

Figure 4. The wetland depression map based on the morphological operators and priori information on the water distribution map.

2.2 Above-water topography reconstruction

The water occurrence map can effectively describe three-dimensional topography at a large spatial scale (Armon et al., 2020; Li et al., 2019b). The water occurrence map is generated by summing the times that the pixel is detected as water and dividing it by the number of total valid observations. Therefore, if there is a accurate water occurrence maps, a close relationship between the water occurrence and the topography for wetland depressions can be found (Li et al., 2021). The open-source Global Surface Water Mapping Layers produced by the European Commission's Joint Research Centre (JRC) contains a water occurrence map, which has been widely used to describe the topography of wetland depressions globally or in different regions (Luo et al., 2019; Pickens et al., 2020; Yao et al., 2019; Zou et al., 2018). However, due to the temporal discontinuity of cloud-free JRC water distribution images, they are more available during dry seasons than wet seasons, leading to deviations in the representation of real topography at the scale of individual wetland depression (Chu et al., 2020).

To address the above issue, this study proposes a method to restore the cloud-contaminated JRC water distribution images to improve the accuracy of the JRC water occurrence map. For wetland depressional areas, the JRC water distribution images are classified into cloud-free and cloud-contaminated images using the cloud screening algorithm of the Google Earth Engine platform. The Canny edge detection algorithm is used to obtain the water body boundary of the two types of images. Theoretically, if the water areas are the same, the water body boundary of the cloud-free image should overlap with the exposed water body boundary in the cloud-contaminated image (Figure 5a). Therefore, by overlapping the water body boundaries of the cloud-free images with the cloud-contaminated images, the missing spatial extent of water bodies in the cloud-contaminated images can be filled.

The corrected JRC water occurrence map is utilized to reconstruct above-water topography. This is because the water occurrence values within the same wetland depression correspond to elevation values (Figure 5b and 5c). However, each corrected water occurrence value may correspond to multiple elevation values in the global DEMs. Therefore, the median of multiple elevation values is used as the unique elevation value corresponding to the water occurrence value.

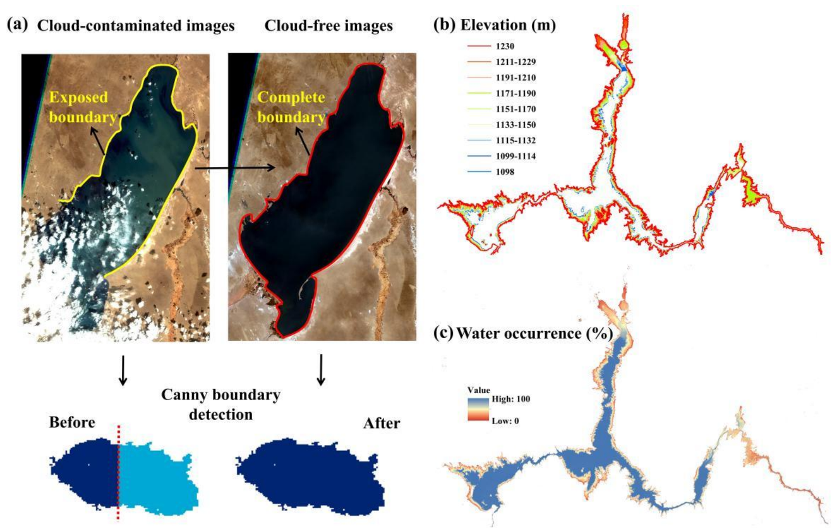

Figure 5. Above-water topography reconstruction of wetland depressional areas. (a) Restoration method of cloud-contaminated JRC water distribution images. (b) LiDAR DEM and JRC water occurrence map of Mead Lakes in the United States.

2.3 Bathymetric information estimation

The remote sensing technologies are used to estimate the underwater bathymetry of wetland depressions, and the similarity between the underwater and above-water hypsometric relationships is served as an evaluation criterion to seek for the optimal solution within the estimated results that accurately represents underwater bathymetry based on the principle of spatial prediction and modeling methods.

The outliers in the underwater are-level pairs are removed using the 3-sigma rule. As the slope profile is a crucial indicator reflecting the hypsometric relationship of wetland depressions (Clark and Shook, 2022; Sjöberg et al., 2022). Therefore, we first form various combinations of the processed underwater area-level pairs (each water area value uniquely corresponds to a water level value in each combination), and calculate the slope profile value p_u for each combination. Then the combination with p_u closest to the above-water slope profile p_a is taken as the optimal solution, which can effectively represent underwater bathymetry of wetland depressions.

In this study, a logarithmic transformation is applied to the calculation formula for the slope profile p of wetland depressions established by Hayashi and Van der Kamp (2000) to obtain Eq. 3. The least squares method is used to solve Eq. 3 to obtain the slope profile p value of wetland depressions:

$$P = \frac{2 \cdot \ln(h_w / h_d)}{\ln(A_w / A_d)} \tag{3}$$

where h (m), A (m^2) represent the depth and area of wetland depressions, and w and d represent the different area-depth pairs.

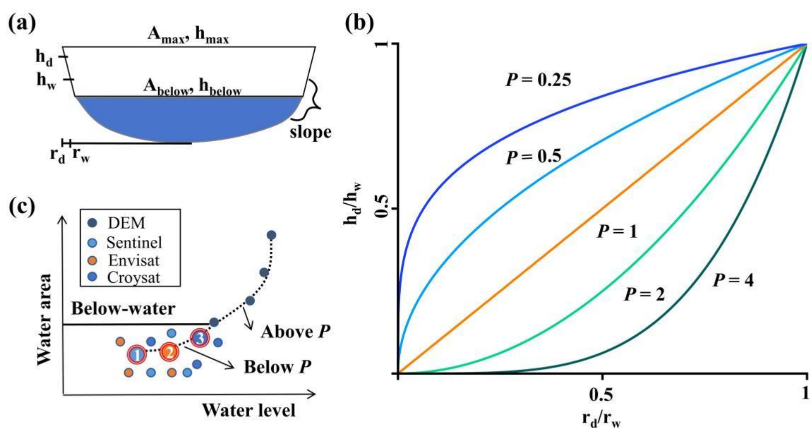

Figure 6. Estimation of bathymetric information for wetland depressional areas. (a) Schematic representation of a simplified wetland depression profile, where h (m), r (m) and A (m^2) represent the depth

https://doi.org/10.5194/hess-2024-71
Preprint. Discussion started: 29 April 2024

Hydrology and Earth System Sciences
Open Access
Discussions

of a wetland depressional area, the distance between the edge and the center of the wetland depression, and the area of the wetland depression, respectively. (b) Wetland depression profile for various *p* values. (c) Methods for bathymetric estimation of wetland depressions, where Sentinel, Envisat, and Croysat are different altimetry satellites, and the numbers 1, 2, and 3 are selected depth-area pairs.

2.4 Estimation of wetland depression water storage capacity

Deriving the area-level hypsometric relationship from the corrected above-water topography and estimated underwater bathymetry of wetland depressions. The monotonic cubic spline and power function are employed to fit the hypsometric relationships (i.e., depth-area relations) to derive the above-water hypsometric curve $f_A(\mathrm{L})$ and the underwater hypsometric curve $f_B(\mathrm{L})$ (Messager et al., 2016; Yao et al., 2018), respectively. Subsequently, the integration of these two curves (Figure 7) is performed to calculate the WDWSC, represented as V in Eq. 4:

$$V = \int_{h_{watersurface}}^{h_{\max}} f_A(\mathrm{L})dL + \int_{0}^{h_{watersurface}} f_B(\mathrm{L})dL \tag{4}$$

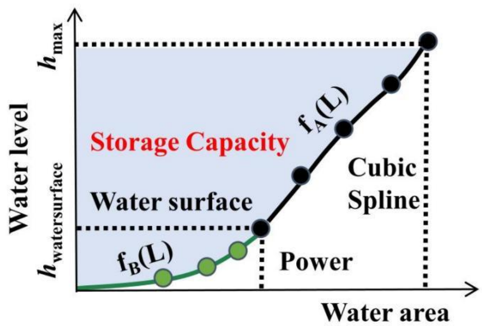

Figure 7. Schematic diagram for the estimation of wetland depression water storage capacity. Two depth-area rating curves are applied for the bathymetric volume and the above-water topographic volume.

3 Validation sites and datasets

3.1 Validation sites

We applied the WetlandSCB to two wetlands in the Nenjiang River Basin (NRB), northeast China, to validate the framework. Draining a total area of 297,100 km^2, the NRB is one of the largest river basins in north China. In this river basin, agricultural lands and wetlands (lakes and swamps) are prevalent (Wu et al., 2023). Recognised as critical regulators of the water balance within the NRB, wetlands are considered more important than other ecosystems in mitigating future hydrological extremes and increasing water availability for agriculture (Chen et al., 2020, Wu et al., 2020a, Wu et al., 2020b, Wu et al., 2020c). For method validation and application of the WetlandSCB framework, we focused on two national nature reserves within the NRB: the Baihe Lake and the Chagan Lake. The Baihe Lake, characterised as a marsh wetland, covers approximately 40 km^2, predominantly comprising seasonal inundation zones, with an average water depth of less than 1 m. In contrast, The Chagan Lake is a large lacustrine wetland of about 372 km^2, mainly composed of perennial inundation zones, with an average water depth of 2.5 m. These two validation wetlands represent different characteristics in terms of type, area, and average water depth to verify the application robustness of our developed framework. Field measurements of topographic and bathymetric information (elevation and depth) were conducted for both the Baihe Lake and the Chagan Lake, consisting of 248 and 657 measurement points, respectively (Figure 8).

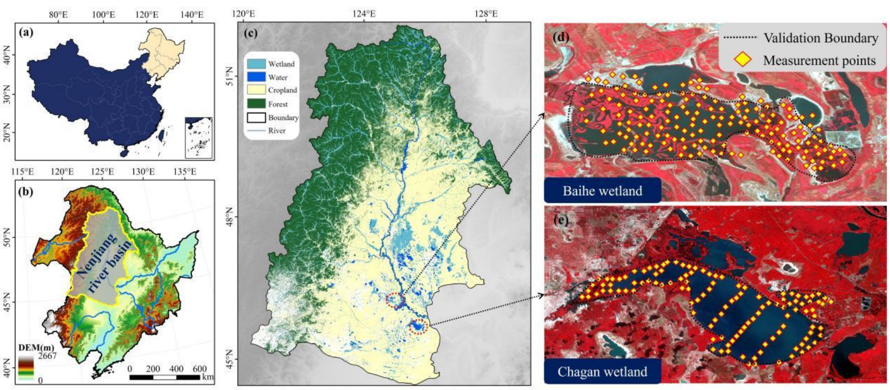

Figure 8. Locations and distribution of elevation and depth measurements across the Baihe Lake and Chagan Lake in the Nenjiang River basin, northeast China.

3.2 Datasets

The application of the WetlandSCB framework requires the following data: (i) the global DEMs sourced from SRTM DEM, with water distribution map sourced from the accompanying SRTM Water Body Data (https://earthexplorer.usgs.gov/); (ii) wetland maps extracted from the 30-m resolution land cover data for the years 1990-2019 (https://zenodo.org/records/5816591, Yang and Huang, 2021) and 30-m resolution wetland map in 2015 year (http://northeast.geodata. cn/index. html, Mao et al., 2020). This study overlays the data from both sources to reduce the uncertainties in the wetland maps; (iii) water distribution maps and water occurrence map obtained from the Global Surface Water datasets

https://doi.org/10.5194/hess-2024-71
Preprint. Discussion started: 29 April 2024

(https://earthengine.google.com, Pekel et al., 2016); (iv) altimetry satellite data sourced from the Sentinel-3A/3B products (https://scihub.copernicus.eu/). In addition, pre-processing of Sentinel-3 altimetry data is performed using the geophysical and atmospheric correction method developed by Huang et al. (2019) (Eq. 5 and Eq. 6) to improve data accuracy:

$$H_{waterlevel} = H_{alt} - R - Cor \tag{5}$$

where $H_{waterlevel}$ is the water level referenced to the EGM96 geoid, H_{alt} is the altitude of the altimeter derived from the modeling of satellite trajectory, R is the range computed through the time duration of the echoes, and Cor is referred to as the geophysical and environmental corrections:

$$Cor = C_{dry} + C_{wet} + C_{iono} + C_{solidEarth} + C_{pole} + C_{EGM96} \tag{6}$$

where C_{dry}, C_{wet}, C_{iono}, $C_{solidEarth}$, C_{pole} and C_{EGM96} are the dry tropospheric, wet tropospheric, ionospheric corrections, the solid Earth tide, polar tide corrections and the EGM96 geoid respectively.

4 Results and discussions

4.1 Performance evaluation of wetland depression spatial delineation and uncertainty analysis

The performance of wetland depression spatial delineation based on the WetlandSCB framework was evaluated using four indicators: overall accuracy, kappa coefficient, producer's accuracy, and user's accuracy (Fig. 9a-f). The results indicate that the WetlandSCB framework can accurately determine the spatial distribution of wetland depressions, with all four indicators exceeding 0.95. In contrast, the user's accuracy is above 0.93 in both validation wetlands (error of commission is 0.07), and the producer's accuracy is only 0.37 (error of omission is 0.63) in Baihe Lake based on the priority-flood algorithm. The findings suggest that the algorithm can effectively identify wetland depressions, but is limited by the numerical errors of the global DEMs, which leads to lower extraction accuracy of the spatial distribution of wetland depressions (Zhou et al., 2016). In comparison, the WetlandSCB framework outperforms the priority-flood algorithm in wetland depression spatial delineation.

Uncertainty in wetland depression spatial delineation using the WetlandSCB framework primarily mainly arises from morphological operators and prior information on water distribution map. Figures 9g and 9h show that, compared with morphological operators, prior information on water distribution map can significantly alter the performance of wetland depression spatial delineation and is a key factor in determining the level of uncertainty. For instance, in Baihe Lake, the overall accuracy and kappa coefficient improved by 0.29 and 0.56, respectively, after processing with prior information on

https://doi.org/10.5194/hess-2024-71
Preprint. Discussion started: 29 April 2024

water distribution map. Similar studies have also found that the type and reliability of prior information are major factors affecting the spatial filling performance of surface water maps (Aires, 2020; Pulvirenti et al., 2011b). Therefore, this study compared the wetland depression spatial delineation results based on three sets of prior information on water distribution map: GLC-FCS30 (from Zhang et al., 2021), CLCD (from Yang and Huang, 2021), and JRC (Fig. 9i and 9j). The overall accuracy differences for the Baihe Lake and Chagan Lake ranged from 0.68 to 0.98 and from 0.93 to 0.99, respectively. In general, the accuracy levels of prior information from high to low were JRC > GLC-FCS30 > CLCD. This suggests that selecting highly reliable prior information on water distribution map is an essential way to reduce uncertainty in the WetlandSCB framework.

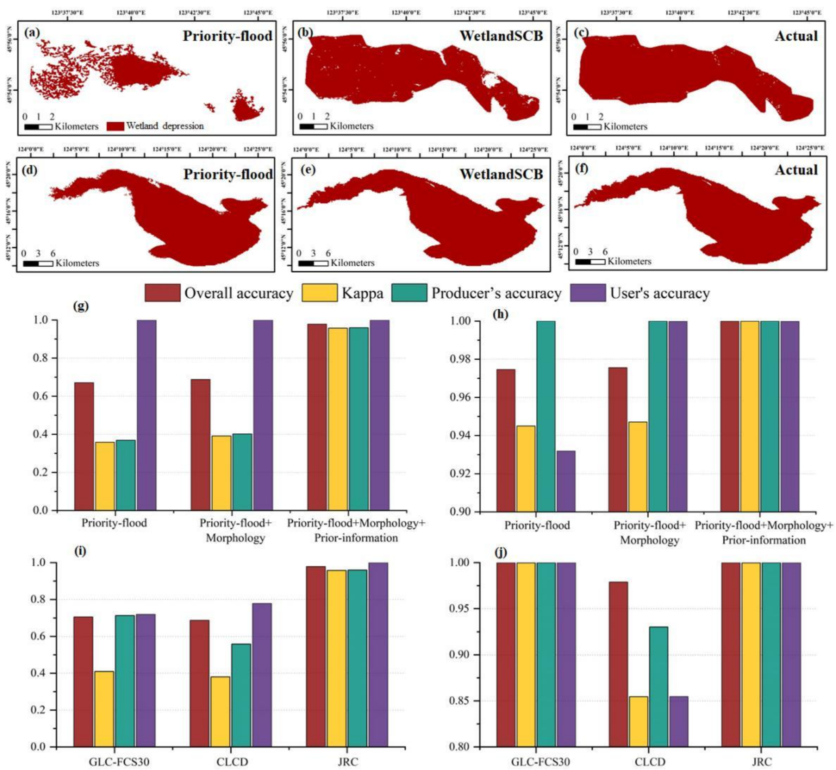

Figure 9. (a), (b), and (c) depict the spatial distribution of wetland depressional areas in the Baihe Lake based on the priority-flood algorithm, WetlandSCB framework, and field measurements, respectively. (d), (e), and (f) show the corresponding results for the Chagan Lake. The impact of morphological operators and prior information on water distribution map from the WetlandSCB framework is illustrated in (g) and (h). The influence of different prior information on water distribution map from the WetlandSCB framework is

https://doi.org/10.5194/hess-2024-71
Preprint. Discussion started: 29 April 2024

Hydrology and Earth System Sciences Discussions
Open Access

presented in (i) and (j).

4.2 Performance evaluation of above-water topography correction and uncertainty analysis

The consistency between the original and corrected above-water topography and the actual above-water topography obtained from field measurements can be evaluated using Pearson correlation coefficients and R^2. The results indicate that the consistency between the original and actual above-water topography is remarkably low, with R^2 values less than 0.2 for both validation wetlands. Previous studies have also observed significant numerical discrepancies between the original and actual above-water topography in some regions (e.g., Mukul et al., 2017; Uuemaa et al., 2020). Compared to the original results, the consistency between the corrected and actual above-water topography significantly improves. For example, the Pearson correlation coefficient and R^2 reach -0.74 and 0.55 in the Baihe Lake, respectively, demonstrating that the WetlandSCB framework can effectively correct numerical biases in above-water topography.

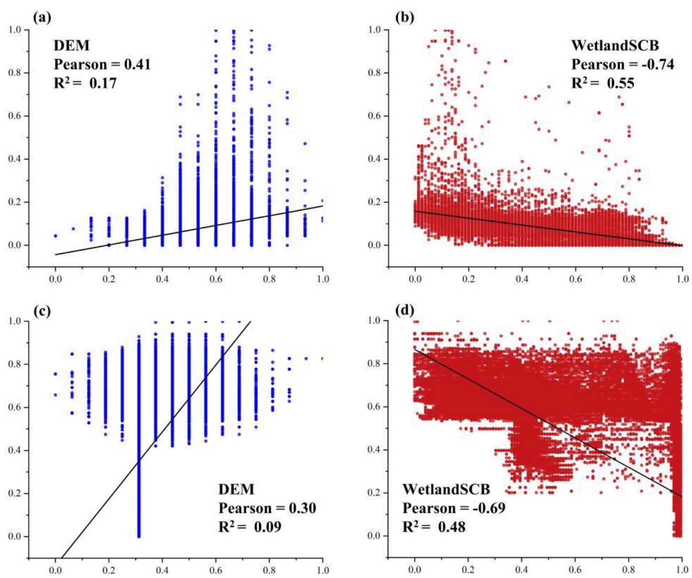

Figure 10. (a) and (b) Consistency analysis results between the original and corrected above-water topography for Baihe Lake. (c) and (d) are corresponding results for Chagan Lake.

Uncertainty in correcting above-water topography using the WetlandSCB framework depends primarily on the accuracy of the water occurrence map. Therefore, this study analyzed the correlation

https://doi.org/10.5194/hess-2024-71
Preprint. Discussion started: 29 April 2024

between two sets of global-scale water occurrence maps, namely GLAD (Pickens et al., 2020) and JRC, with actual above-water topography. The results show that the correlation level of GLAD is superior to JRC in the Baihe Lake, while the opposite is observed in the Chagan Lake. Additionally, the R^2 values for both sets of water occurrence maps are less than 0.4 (Figure 11c-f), which is significantly lower than the accuracy level of the corrected above-water topography. This clearly shows the superiority of the water occurrence map generated by the WetlandSCB framework over the GLAD or original JRC map.

It is to note that the water occurrence map generated by the WetlandSCB framework still has a certain level of uncertainty. First, the extraction of a complete and accurate water spatial distribution from cloud-free images is constrained by factors such as the classification algorithm (Figure 11a) (Peket et al., 2016), but some correction algorithms have been proposed to enhance raw water distribution images (Zhao and Gao, 2018). Second, there is currently a lack of high-precision, temporally and spatially continuous water distribution maps (Figure 11b). Future efforts could include the use of image fusion methods, such as the Spatial and Temporal Adaptive Reflectance Fusion Mode, to fuse data from multi-source remote sensing products such as Sentinel-2, MODIS, and Landsat, which can effectively enhance the accuracy of water occurrence map (He et al., 2020; Wang et al., 2016).

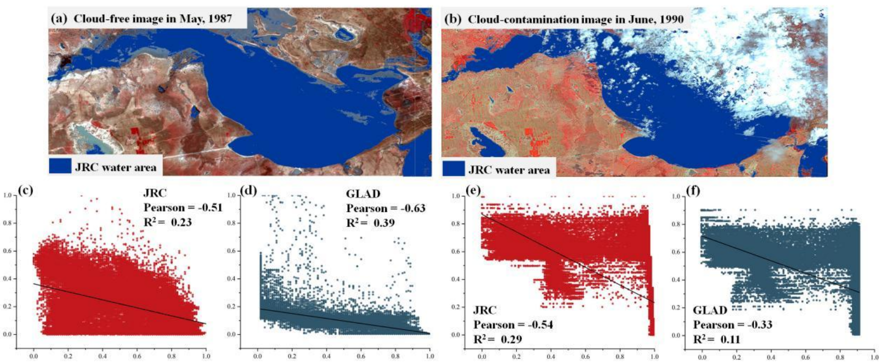

Figure 11. (a) and (b) depict sources of uncertainty in water occurrence map generated by the WetlandSCB framework. (c), (d), (e) and (f) illustrate the difference between two water occurrence maps on the performance of above-water topography correction in the Baihe Lake and the Chagan Lake.

4.3 Performance evaluation of bathymetric information estimation

The slope profile p is used to describe the bathymetry of wetland depressional areas. The calculated p values for the Baihe lake and the Chagan Lake using the WetlandSCB framework are 7.45 and 4.08, respectively. The relative errors with respect to the actual p values obtained from field measurements are both less than 3%, demonstrating the high accuracy of the framework in estimating underwater bathymetry.

To further prove the superiority of the WetlandSCB framework in estimating bathymetry, this study employed spatial prediction and modeling methods, resulting in a p value of 8.65 for the Baihe Lake and 4.78 for the Chagan Lake. The relative errors with respect to the actual p values are both greater than 18%, indicating that this method may lead to substantial errors in some regions, as also reported by Papa et al. (2013) and Vanthof and Kelly. (2019). Furthermore, previous studies have often applied smoothing methods to the global DEMs to enhance the accuracy of topographic characterization in wetland depressions (e.g., Jones et al., 2018; Wu et al., 2019). In this regard, we further used the Gaussian-smoothed global DEMs and the spatial prediction and modelling methods to calculate p for the Baihe Lake and the Chagan Lake. The resulting values were 8.51 and 4.37, with relative errors of 17.63% and 7.9%, respectively. This underscores that smoothing methods do indeed contribute to improving the accuracy of topographic information in wetland depressions. Notably, the relative error for the Chagan Lake is significantly lower than that for the Baihe Lake, which is consistent with the findings of Liu and Song (2022), who reported that the spatial prediction and modeling methods are suitable for wetlands with long and narrow shape. In summary, it can be seen that the WetlandSCB framework excels in the accuracy of estimating bathymetry in wetland depressional areas when compared to other methods.

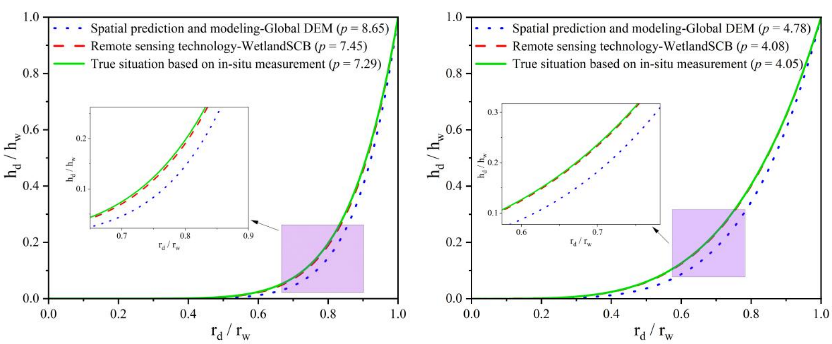

Figure 12. Slope profile p values of wetland depressions for the Baihe Lake (left) and the Chagan Lake

https://doi.org/10.5194/hess-2024-71
Preprint. Discussion started: 29 April 2024

(right), calculated with spatial prediction and modeling methods, and the WetlandSCB framework in comparison with filed measurements.

4.4 WetlandSCB framework application and implications for integrated water resources management

Wetland depressions are largely disregarded in many hydrologic modeling practices. Rare studies exist on how their exclusion can lead to potentially inaccurate model projections and understanding of hydrologic dynamics across the world's river basins (Rajib et al., 2020). This study applied a novel framework delineating the topography and bathymetry of wetland depressional areas and focusing on two distinctive wetlands to estimate WDWSC. Using the field measurements of topography and bathymetry of the Baihe Lake and the Chagan Lake, the depth-area hypsometric curves were constructed, and the WDWSC of the Baihe Lake and the Chagan Lake were estimated to be 61 million m^3 and 526 million m^3, respectively (Fig. 13). The estimation results based on the WetlandSCB framework were correspondingly 55 million m^3 and 521 million m^3, and the relative errors with the actual measured WDWSC were both less than 10%, which is a good level of accuracy in estimation precision (Moriasi et al., 2015). These results demonstrate the ability of the framework to accurately estimate WDWSC, which can be applied to regions lacking field measurement data for global-scale wetland water storage capacity estimation.

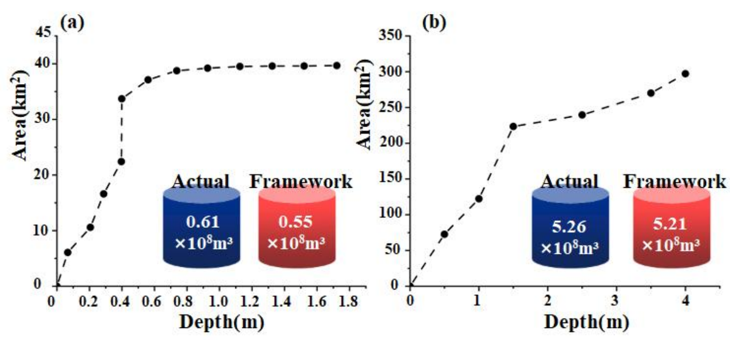

Figure 13. The dashed line and blue cylinder represent the actual hypsometric curve and the corresponding actual WDWSC based on field measurements, respectively. The red cylinder indicates the estimated WDWSC from the WetlandSCD framework for the Baihe Lake (a) and the Chagan Lake (b).

https://doi.org/10.5194/hess-2024-71
Preprint. Discussion started: 29 April 2024

Wetlands play a pivotal role in mitigating flood and drought risks, as well as addressing water scarcity challenge within a river basin. Previous studies underscore the significant impact of wetlands in attenuating future flood characteristics, including peak flows, mean flows, duration, and flow volume for various return period floods (Wu et al., 2023). Concurrently, wetlands contribute to enhancing baseflow during both summer and winter seasons in the NRB (Wu et al., 2020c). Given the NRB is a agriculture-dominated river basin, wetlands serves as the main water supply nodes by collecting the flash flood and storing and purifying irrigation return flows. This reclaimed water can be efficiently reused for irrigation purposes in the NRB (Meng et al., 2019; Smiley and Allred, 2011; Zou et al., 2018). The WDWSC is a key parameter for evaluating the flood control and water supply capacity of wetlands, also as a important prerequisite for understanding the impact of wetlands on extreme hydrological events (Acreman and Holden, 2013). Therefore, the developed WetlandSCB framework, which can provide accurate estimation of the WDWSC, contributes to the management of food and water security in the NRB. Against the backdrop of global environmental change, characterized by an escalation in the intensity and frequency of extreme hydrological events, and the increasing disparity between water resource supply and demand, there is an urgent need for a novel integrated water resources management approach based on natural solutions (Rodell and Li, 2023; Thorslund et al., 2017; Yin et al., 2018). Wetlands have emerged as a nature-based solution in various water resources management practices (Ferreira et al., 2023). Taking advantage of the wetland hydrological regulation functions is instrumental in addressing the risks of flood and drought disasters arising from global climate change, land use change, as well as the water scarcity risks stemming from agricultural-ecological water competition. This can help develop effective adaptation strategies and decisions for integrated water resources management.

5 Conclusions

This study developed a novel framework to accurately quantify wetland depression water storage capacity using coarse-resolution terrain data. The developed framework, WetlandSCB integrates multi-source remote sensing data, historical maps and prior knowledge, and achieved a high prediction of wetland depressional distribution and water storage capacity. This is achieved through four steps: 1) integrating priority-flood algorithm, morphological operators and prior information on water distribution maps to delineate spatial extent of wetland depressional areas; 2) correcting numerical biases in above-water topography with water occurrence map; 3) coupling spatial prediction and

https://doi.org/10.5194/hess-2024-71
Preprint. Discussion started: 29 April 2024

Hydrology and Earth System Sciences
Open Access
Discussions

modeling with remote sensing techniques to estimate bathymetric information, and 4) quantifying depressional area water storage capacity based on depth-area rating curves. The concept and technical approaches are applicable to large-scale wetland depression water storage estimation, as well as to the regions where field measurements and/or high-resolution data are not available. Application of the WetlandSCB framework provides accurate distribution and depth-area relations of wetland depressional areas which can be incorporated into wetland modules of hydrological models (e.g., HYDROTEL, SWAT, HYPE, CHRM) to improve the accuracy of flow and storage predictions in river basins.

Data Availability.

The data used in this study are openly available for research purposes. The SRTM DEM and SRTM Water Body Data can be downloaded at https://earthexplorer.usgs.gov. Wetland maps are available at https://zenodo.org/records/5816591 and http://northeast.geodata. cn/index. html. Water distribution maps and water occurrence map are available at https://earthengine.google.com. Altimetry satellite data can be downloaded at https://scihub.copernicus.eu.

Author contribution.

Boting Hu, Liwen chen and Yanfeng Wu designed and executed the study, all authors contributed to general idea, the discussion and editing of the manuscript.

Competing interest.

The authors declare that they have no conflict of interest.

Acknowledgments.

This work was supported by the Strategic Priority Research Program of the Chinese Academy of Sciences, China (XDA28020501), National Natural Science Foundation of China (41877160), National Key Research and Development Program of China (2017YFC0406003, 2021YFC3200203) and The Consulting Project Proposal of the Chinese Academy of Engineering (JL2023-17).

References

Acreman, M. and Holden, J.: How wetlands affect floods, Wetlands, 33, 773-786, https://doi.org/10.1007/s13157-013-0473-2, 2013.

Ahmad, S. K., Hossain, F., Pavelsky, T., Parkins, G. M., Yelton, S., Rodgers, M., Little, S., Haldar, D., Ghafoor, S., Khan, R. H., Shawn, N. A., Haque, A., and Biswas, R. K.:Understanding volumetric water storage in monsoonal wetlands of Northeastern Bangladesh, Water Resour. Res, 56(12), e2020WR027989, https://doi.org/10.1029/2020WR027989, 2020.

Aires, F., Miolane, L., Prigent, C., Pham, B., Fluet-Chouinard, E., Lehner, B., and Papa, F.: A global dynamic long-term inundation extent dataset at high spatial resolution derivedthrough downscaling of satellite observations, J. Hydrometeorol, 18(5), 1305-1325, https://doi.org/10.1175/JHM-D-16-0155.1, 2017.

Armon, M., Dente, E., Shmilovitz, Y., Mushkin, A., Cohen, T. J., Morin, E., and Enzel, Y.:Determining bathymetry of shallow and ephemeral desert lakes using satellite imagery andaltimetry, Geophys. Res. Lett, 47(7), e2020GL087367, https://doi.org/10.1029/2020GL087367, 2020.

Barnes, R., Lehman, C., and Mulla, D.: Priority-flood: An optimal depression-filling and watershed-labeling algorithm for digital elevation models, Comput. Geosci, 62, 117-127, https://doi.org/10.1016/j.cageo.2013.04.024, 2014.

Bonnema, M., Sikder, S., Miao, Y., Chen, X., Hossain, F., Ara Pervin, I., Mahbubur Rahman, S. M., and Lee, H.: Understanding satellite-based monthly-to-seasonal reservoir outflowestimation as a function of hydrologic controls, Water Resour. Res, 52(5), 4095-4115, https://doi.org/10.1002/2015WR017830, 2016.

Bonnema, M. and Hossain, F.: Inferring reservoir operating patterns across the Mekong Basin using only space observations, Water Resour. Res, 53(5), 3791-3810, https://doi.org/10.1002/2016WR019978, 2017.

Chen, W., Nover, D., Yen, H., Xia, Y., He, B., Sun, W., and Viers, J.: Exploring the multiscale hydrologic regulation of multipond systems in a humid agricultural catchment, WaterRes, 184, 115987, https://doi.org/10.1016/j.watres.2020.115987, 2020.

Chu, L., Oloo, F., Sudmanns, M., Tiede, D., Hölbling, D., Blaschke, T., and Teleoaca, I.: Monitoring long-term shoreline dynamics and human activities in the Hangzhou Bay, China, combining daytime and nighttime EO data, Big Earth Data, 4(3), 242-264, https://doi.org/10.1080/20964471.2020.1740491, 2020.

Clark, M. P. and Shook, K. R.: The Numerical Formulation of Simple Hysteretic Models to Simulate the Large-Scale Hydrological Impacts of Prairie Depressions, Water Resour. Res, 58(12), e2022WR032694, https://doi.org/10.1029/2022WR032694, 2020.

Cohen, M. J., Creed, I. F., Alexander, L., Basu, N. B., Calhoun, A. J., Craft, C., D'Amico, E., DeKeyser, E., Fowler, L., Golden, H. E., Jawitz, J. W., Kalla, P., Kirkman, L. K.,Lane, C. R., Lang, M., Leibowitz, S. G., Lewis, D.B., Marton, J., McLaughlin, D. L., Mushet D. M., Raanan-Kiperwas, H., Rains, M. C., Smith, L., and Walls, S. C.: Do geographically isolated wetlands influence landscape functions?, Proc. Natl. Acad. Sci. U. S.A, 113(8), 1978-1986, https://doi.org/10.1073/pnas.1512650113, 2016.

De Klerk, A. R., De Klerk, L. P., Oberholster, P. J., Ashton, P. J., Dini, J. A., and Holness, S. D.: A review of depressional wetlands (pans) in South Africa, including a water quality classification system, https://doi.org/10.13140/RG.2.2.28486.06723, 2016.

https://doi.org/10.5194/hess-2024-71
Preprint. Discussion started: 29 April 2024

Hydrology and Earth System Sciences
Open Access
Discussions

Duan, Z. and Bastiaanssen, W. G. M.: Estimating water volume variations in lakes and reservoirs from four operational satellite altimetry databases and satellite imagery data, RemoteSens. Environ, 134, 403-416, https://doi.org/10.1016/j.rse.2013.03.010, 2013.

Evenson, G. R., Golden, H. E., Lane, C. R., McLaughlin, D. L., and D'Amico, E.: Depressional wetlands affect watershed hydrological, biogeochemical, and ecological functions, Ecol. Appl, 28(4), 953-966, https://doi.org/10.1002/eap.1701, 2018.

Fang, Y., Li, H., Wan, W., Zhu, S., Wang, Z., Hong, Y., and Wang, H.: Assessment of water storage change in China's lakes and reservoirs over the last three decades, Remote Sens, 11(12), 1467, https://doi.org/10.3390/rs11121467, 2019.

Ferreira, C. S., Kašanin-Grubin, M., Solomun, M. K., Sushkova, S., Minkina, T., Zhao, W.,and Kalantari, Z.: Wetlands as nature-based solutions for water management in different environments, Curr. Opin. Environ. Sci. Health, 100476, https://doi.org/10.1016/j.coesh.2023.100476, 2023.

Gao, H.: Satellite remote sensing of large lakes and reservoirs: From elevation and area tostorage, Wiley Interdisciplinary Reviews: Water, 2(2), 147-157, https://doi.org/10.1002/wat2.1065, 2015.

Haag, K. H., Lee, T. M., Herndon, D. C., County, P., and Water, T. B.: Bathymetry and vegetation in isolated marsh and cypress wetlands in the northern Tampa Bay area, 2000-2004, US Department of the Interior, US Geological Survey, https://lccn.loc.gov/2005452253, 2005.

Hayashi, M. and Van der Kamp, G.: Simple equations to represent the volume–area–depthrelations of shallow wetlands in small topographic depressions, J. Hydrol, 237(1-2), 74-85,https://doi.org/10.1016/S0022-1694(00)00300-0, 2000.

He, D., Zhong, Y., and Zhang, L.: Spectral–spatial–temporal MAP-based sub-pixel mappingfor land-cover change detection, IEEE Trans. Geosci. Remote Sensing, 58(3), 1696-1717, https://doi.or10.1109/TGRS.2019.2947708, 2019.

Huang, Q., Li, X., Han, P., Long, D., Zhao, F., and Hou, A.: Validation and application of water levels derived from Sentinel-3A for the Brahmaputra River, SCI CHINA. TECHNOL SC, 1760-1772, https://doi.org/10.1007/s11431-019-9535-3, 2019.

Huang, S., Young, C., Feng, M., Heidemann, K., Cushing, M., Mushet, D. M., and Liu, S.: Demonstration of a conceptual model for using LiDAR to improve the estimation of floodwater mitigation potential of prairie pothole region wetlands, J. Hydrol, 405(3–4),417–426, https://doi.org/10.1016/j.jhydrol.2011.05.040, 2011.

Jones, C. N., Evenson, G. R., McLaughlin, D. L., Vanderhoof, M. K., Lang, M. W., McCarty, G. W., Golden, E. H., Lane, C.R., and Alexander, L. C.: Estimating restorable wetland water storage at landscape scales, Hydrol. Process, 32(2), 305-313, https://doi.org/10.1002/hyp.11405, 2018.

Kessler, A. C. and Gupta, S. C.: Drainage impacts on surficial water retention capacity ofa prairie pothole watershed, J. Am. Water Resour. Assoc, 1–13, https://doi.org/ 10.1111/jawr.12288, 2015.

Lane, C. R. and D'Amico, E.: Calculating the ecosystem service of water storage in isolated wetlands using LiDAR in North Central Florida, USA, Wetlands, 30, 967-977, https://doi.org/10.1007/s13157-010-0085-z, 2010.

Lane, C. R., Leibowitz, S. G., Autrey, B. C., LeDuc, S. D., and Alexander, L. C.: Hydrological, physical, and chemical functions and connectivity of non-floodplain wetlands to downstrea

https://doi.org/10.5194/hess-2024-71
Preprint. Discussion started: 29 April 2024

m waters: A review, J. Am. Water Resour. Assoc, 54(2), 346-371, https://doi.org/10.1111/1752-1688.12633, 2018.

Lindsay, J. B.: Whitebox GAT: A case study in geomorphometric analysis, Comput. Geosci, 95, 75-84, https://doi.org/10.1016/j.cageo.2016.07.003, 2016.

Liu, K. and Song, C.: Modeling lake bathymetry and water storage from DEM data constrained by limited underwater surveys, J. Hydrol, 604, 127260, https://doi.org/10.1016/j.jhydrol.2021.127260, 2022.

Liu, K., Song, C., Zhan, P., Luo, S., and Fan, C.: A Low-Cost Approach for Lake Volume Estimation on the Tibetan Plateau: Coupling the Lake Hypsometric Curve and Bottom Elevation, Front. Earth Sci, 10, 925944, https://doi.org/10.3389/feart.2022.925944, 2022.

Liu, K., Song, C., Zhao, S., Wang, J., Chen, T., Zhan, P., Fan, C., and Zhu, J.: Mapping inundated bathymetry for estimating lake water storage changes from SRTM DEM: A global investigation., Remote Sens. Environ, 301, 113960, https://doi.org/10.1016/j.rse.2023.113960, 2024.

Li, X., Ling, F., Foody, G. M., Boyd, D. S., Jiang, L., Zhang, Y., Zhou, P., Wang, Y., Chen, R., and Du, Y.: Monitoring high spatiotemporal water dynamics by fusing MODIS, Landsat, water occurrence data and DEM, Remote Sens. Environ, 265, 112680, https://doi.org/10.1016/j.rse.2021.112680, 2021.

Li, X., Long, D., Huang, Q., Han, P., Zhao, F., and Wada, Y.: High-temporal-resolution water level and storage change data sets for lakes on the Tibetan Plateau during 2000–2017using multiple altimetric missions and Landsat-derived lake shoreline positions, Earth Syst. Sci. Data, 11(4), 1603-1627, https://doi.org/10.5194/essd-11-1603-2019, 2019a.

Li, Y., Gao, H., Jasinski, M. F., Zhang, S., and Stoll, J. D.: Deriving high-resolution reservoir bathymetry from ICESat-2 prototype photon-counting lidar and landsat imagery, IEEE Trans. Geosci. Remote Sensing, 57(10), 7883-7893, https://doi.org/10.1109/TGRS.2019.2917012, 2019b.

Luo, S., Song, C., Liu, K., Ke, L., and Ma, R.: An effective low-cost remote sensing approach to reconstruct the long-term and dense time series of area and storage variations forlarge lakes, Sensors, 19(19), 4247, https://doi.org/10.3390/s19194247, 2019.

Mao, D., Wang, Z., Du, B., Li, L., Tian, Y., Jia, M., Zeng, Y., Song, K. Jiang, M., and Wang, Y.: National wetland mapping in China: A new product resulting from object-based and hierarchical classification of Landsat 8 OLI images, ISPRS-J. Photogramm. Remote Sens, 164, 11-25, https://doi.org/10.1016/j.isprsjprs.2020.03.020, 2020.

Meng, B., Liu, J. L., Bao, K., and Sun, B.: Water fluxes of Nenjiang River Basin with ecological network analysis: Conflict and coordination between agricultural development andwetland restoration, J. Clean Prod, 213, 933-943, https://doi.org/10.1016/j.jclepro.2018.12.243,2019.

Messager, M. L., Lehner, B., Grill, G., Nedeva, I., and Schmitt, O.: Estimating the volume and age of water stored in global lakes using a geo-statistical approach, Nat. Commun, 7, 13603, https://doi.org/10.1038/ncomms13603, 2016.

Moriasi, D. N., Gitau, M. W., Pai, N., and Daggupati, P.: Hydrologic and water quality models: Performance measures and evaluation criteria, Trans. ASABE, 58(6), 1763-1785, https://doi.org/10.13031/trans.58.10715, 2015.

Mukul, M., Srivastava, V., Jade, S., and Mukul, M.: Uncertainties in the shuttle radar topography mission (SRTM) Heights: Insights from the indian Himalaya and Peninsula, Sci Rep, 7(1), 41672, https://doi.org/10.1038/srep41672, 2017.

https://doi.org/10.5194/hess-2024-71
Preprint. Discussion started: 29 April 2024

Papa, F., Frappart, F., Güntner, A., Prigent, C., Aires, F., Getirana, A. C., and Maurer, R.:Surface freshwater storage and variability in the Amazon basin from multi-satellite observations, 1993–2007, J. Geophys. Res.-Atmos, 118(21), 11-951, https://doi.org/10.1002/2013JD020500, 2013.

Pekel, J. F., Cottam, A., Gorelick, N., and Belward, A. S.: High-resolution mapping of global surface water and its long-term changes, Nature, 540(7633), 418-422, https://doi.org/10.1038/nature20584, 2016.

Pickens, A. H., Hansen, M. C., Hancher, M., Stehman, S. V., Tyukavina, A., Potapov, P., Marroquin, B., and Sherani, Z.: Mapping and sampling to characterize global inland waterdynamics from 1999 to 2018 with full Landsat time-series, Remote Sens. Environ, 243,111792, https://doi.org/10.1016/j.rse.2020.111792, 2020.

Pulvirenti, L., Chini, M., Pierdicca, N., Guerriero, L., and Ferrazzoli, P.: Flood monitoringusing multi-temporal COSMO-SkyMed data: Image segmentation and signature interpretation, Remote Sens. Environ, 115(4), 990-1002, https://doi.org/10.1016/j.rse.2010.12.002, 2011a.

Pulvirenti, L., Pierdicca, N., Chini, M., and Guerriero, L.: An algorithm for operational flood mapping from Synthetic Aperture Radar (SAR) data using fuzzy logic, Nat. Hazards Earth Syst. Sci, 11(2), 529-540, https://doi.org/10.5194/nhess-11-529-2011, 2011b.

Rajib, A., Golden, H. E., Lane, C. R., and Wu, Q.: Surface depression and wetland waterstorage improves major river basin hydrologic predictions, Water Resour. Res, 56(7), e2019WR026561, https://doi.org/10.1029/2019WR026561, 2020.

Rodell, M. and Li, B.: Changing intensity of hydroclimatic extreme events revealed by GRACE and GRACE-FO, Nat. Water, 1(3), 241-248, https://doi.org/10.1038/s44221-023-00040-5, 2023.

Shook, K., Papalexiou, S., and Pomeroy, J. W.: Quantifying the effects of Prairie depressional storage complexes on drainage basin connectivity, J. Hydrol, 593, 125846, https://doi.org/10.1016/j.jhydrol.2020.125846, 2021.

Sjöberg, Y., Dessirier, B., Ghajarnia, N., Jaramillo, F., Jarsjö, J., Panahi, D. M., Xu, D., Zou, L., and Manzoni, S.: Scaling relations reveal global and regional differences in morphometry of reservoirs and natural lakes, Sci. Total Environ, 822, 153510, https://doi.org/10.1016/j.scitotenv.2022.153510, 2022.

Smiley Jr, P. C. and Allred, B. J.: Differences in aquatic communities between wetlands created by an agricultural water recycling system, Wetl. Ecol. Manag, 19(6), 495-505, https://doi.org/10.1007/s11273-011-9231-5, 2011.

Thorslund, J., Jarsjo, J., Jaramillo, F., Jawitz, J. W., Manzoni, S., Basu, N. B., Chalov, M.J., Creed, I. F., Goldenberg, R., Hylin, A., Kalantari, Z., Koussis, A. D., Lyon, S. W., Mazi, K., Mard, J., Persson, K., Pietro, J., Prieto, C., Quin, A., and Destouni, G.: Wetlands as large-scale nature-based solutions: Status and challenges for research, engineeringand management, Ecol. Eng, 108, 489-497, https://doi.org/10.1016/j.ecoleng.2017.07.012, 2017.

Tsai, J. S., Venne, L. S., McMurry, S. T., and Smith, L. M.: Vegetation and land use impact on water loss rate in playas of the Southern High Plains, USA, Wetlands, 30, 1107-1116, https://doi.org/10.1007/s13157-010-0117-8, 2010.

Uuemaa, E., Ahi, S., Montibeller, B., Muru, M., and Kmoch, A.: Vertical accuracy of freely available global digital elevation models (ASTER, AW3D30, MERIT, TanDEM-X, SRTM,and NASADEM), Remote Sens, 12(21), 3482, https://doi.org/10.3390/rs12213482, 2020.

Vanthof, V. and Kelly, R.: Water storage estimation in ungauged small reservoirs with the TanDEM-X DEM and multi-source satellite observations, Remote Sens. Environ, 235, 111437, https://doi.org/10.1016/j.rse.2019.111437, 2019.

Verones, F., Pfister, S., and Hellweg, S.: Quantifying area changes of internationally important wetlands due to water consumption in LCA, Environ. Sci. Technol, 47(17), 9799-9807, https://doi.org/10.1021/es400266v, 2013.

Wang, Q., Shi, W., and Atkinson, P. M.: Spatiotemporal subpixel mapping of time-series images, IEEE Trans. Geosci. Remote Sensing, 54(9), 5397-5411, https://doi.org/10.1109/TGRS.2016.2562178, 2016.

Wu, Q., Lane, C. R., Wang, L., Vanderhoof, M. K., Christensen, J. R., and Liu, H.: Efficient delineation of nested depression hierarchy in digital elevation models for hydrological analysis using level-set method, J. Am. Water Resour. Assoc, 55(2), 354-368, https://doi.org/10.1111/1752-1688.12689, 2019.

Wu, Q. and Lane, C. R.: Delineation and quantification of wetland depressions in the Prairie Pothole Region of North Dakota, Wetlands, 36(2), 215-227, https://doi.org/10.1007/s13157-015-0731-6, 2016.

Wu, Y., Sun, J., Blanchette, M., Rousseau, A. N., Xu, Y. J., Hu, B., and Zhang, G.: Wetland mitigation functions on hydrological droughts: From drought characteristics to propagation of meteorological droughts to hydrological droughts, J. Hydrol, 617, 128971, https://doi.org/10.1016/J.JHYDROL.2022.128971, 2023.

Wu, Y., Sun, J., Xu, Y. J., Zhang, G., and Liu, T.: Projection of future hydrometeorological extremes and wetland flood mitigation services with different global warming levels: A case study in the Nenjiang river basin, Ecol. Indic, 140, 108987, https://doi.org/10.1016/j.ecolind.2022.108987, 2022a.

Wu, Y., Zhang, G., Rousseau, A. N., and Xu, Y. J.: Quantifying streamflow regulation services of wetlands with an emphasis on quickflow and baseflow responses in the Upper Nenjiang River Basin, Northeast China, J. Hydrol, 583, 124565, https://doi.org/10.1016/j.jhydrol.2020.124565, 2020b.

Wu, Y., Zhang, G., Rousseau, A. N., Xu, Y. J., and Foulon, É.: On how wetlands can provide flood resilience in a large river basin: a case study in Nenjiang river Basin, China, J.Hydrol, 587, 125012, https://doi.org/10.1016/j.jhydrol.2020.125012, 2020c.

Xiong, L., Tang, G., Yang, X., and Li, F.: Geomorphology-oriented digital terrain analysis:Progress and perspectives, J. Geogr. Sci, 31, 456-476, https://doi.org/10.1007/s11442-021-1853-9, 2021.

Yang, J. and Huang, X.: 30 m annual land cover and its dynamics in China from 1990 to 2019, Earth Syst. Sci. Data, 2021, 1-29. https://doi.org/10.5194/essd-13-3907-2021, 2021.

Yao, F., Wang, J., Wang, C., and Crétaux, J. F.: Constructing long-term high-frequency time series of global lake and reservoir areas using Landsat imagery, Remote Sens. Environ, 232, 111210, https://doi.org/10.1016/j.rse.2019.111210, 2019.

Yao, F., Wang, J., Yang, K., Wang, C., Walter, B. A., and Crétaux, J. F.: Lake storage variation on the endorheic Tibetan Plateau and its attribution to climate change since the newmillennium, Environ. Res. Lett, 13(6), 064011, https://doi.org/10.1088/1748-9326/aab5d3,2018.

https://doi.org/10.5194/hess-2024-71
Preprint. Discussion started: 29 April 2024

Hydrology and Earth System Sciences
Open Access
Discussions

Yin, J., Gentine, P., Zhou, S., Sullivan, S. C., Wang, R., Zhang, Y., and Guo, S.: Large increase in global storm runoff extremes driven by climate and anthropogenic changes, Nat.Commun, 9(1), 4389, https://doi.org/10.1038/s41467-018-06765-2, 2018.

Zhang, X., Liu, L., Chen, X., Gao, Y., Xie, S., and Mi, J.: GLC_FCS30: Global land-cover product with fine classification system at 30 m using time-series Landsat imagery, EarthSyst. Sci. Data, 13(6), 2753-2776, https://doi.org/10.5194/essd-13-2753-2021, 2021.

Zhao, G. and Gao, H.: Automatic correction of contaminated images for assessment of reservoir surface area dynamics, Geophys. Res. Lett, 45(12), 6092-6099, https://doi.org/10.1029/2018GL078343, 2018.

Zhou, G., Sun, Z., and Fu, S.: An efficient variant of the priority-flood algorithm for filling depressions in raster digital elevation models, Comput. Geosci, 90, 87-96, https://doi.org/10.1016/j.cageo.2016.02.021, 2016.

Zou, Y., Wang, L., Xue, Z., E, M., Jiang, M., Lu, X., Yang, S., Shen, X., Liu, Z., Sun, G., and Yu, X.: Impacts of agricultural and reclamation practices on wetlands in the AmurRiver Basin, Northeastern China, Wetlands, 38, 383-389, https://doi.org/10.1007/s13157-017-0975-4, 2018.

Zou, Z., Xiao, X., Dong, J., Qin, Y., Doughty, R. B., Menarguez, M. A., Zhang, C., and Wang, J.: Divergent trends of open-surface water body area in the contiguous United States from 1984 to 2016, Proc. Natl. Acad. Sci. U. S. A, 115(15), 3810-3815, https://doi.org/10.1073/pnas.1719275115, 2018.